

Electronic Supplementary Material (ESI) for Dalton Transactions.
This journal is © The Royal Society of Chemistry 2018

Novel Luminescent homo/heterometallic platinum(II) alkynyl complexes based on a Y-shaped pyridyl diphosphine

Li-Jing Han, Xiu-Xin Wu, Zheng-Gen Ma, Yi Li, Qiao-Hua Wei**

^a MOE Key Laboratory for Analytical Science of Food Safety and Biology, Fujian Provincial Key Laboratory of Analysis and Detection Technology for Food Safety, Fujian Provincial Key Laboratory of Electrochemical Energy Storage Materials, College of Chemistry, Fuzhou University, Fuzhou, Fujian 350108, China.

^b State Key Laboratory of Structural Chemistry, Fujian Institute of Research on the Structure of Matter and Graduate School of CAS, Fuzhou, Fujian 350002, China.

E-mail: qhw76@fzu.edu.cn; liy99@fzu.edu.cn.

Table of Contents

content	page
Cover page	1
Table of Contents	2
Characterizations (Fig. S1-S2)	3-4
Crystal Structures (Table S1-S4)	5-8
Photophysical Properties (Table S5-S6, Fig. S3-S7)	9-15
References	16

Characterizations

Additional IR Analysis

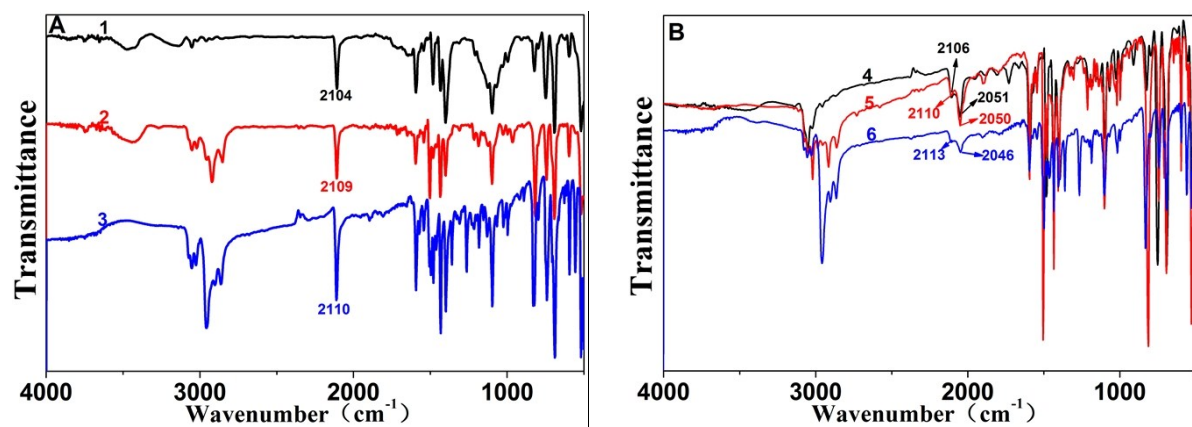


Fig. S1 FTIR spectra of complexes **1-3** (A) and **4-6** (B).

Characterizations

Additional $^{31}\text{P}\{\text{H}\}$ NMR Analysis

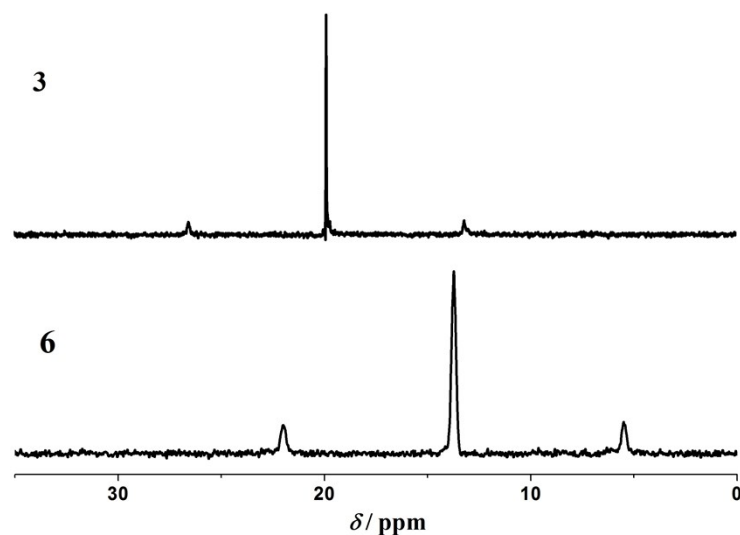


Fig. S2 $^{31}\text{P}\{\text{H}\}$ NMR spectra for complex 3 and 6 in CDCl_3 solution.

Crystal Structures

Table S1. Crystal data and structure refinement for **1·3/2CH₂Cl₂** and **3·MeCN·CH₂Cl₂**.

Compound	1·3/2CH₂Cl₂	3·MeCN·CH₂Cl₂
Empirical formula	C ₂₀₇ H ₁₅₄ Cl ₆ N ₄ P ₈ Pt ₄	C ₁₂₃ H ₁₁₂ Cl ₂ N ₄ P ₄ Pt ₂
fw	3938.15	2231.13
Temperature (K)	193 (2)	193 (2)
radiation (λ , Å)	0.72000	0.72000
Crystal system	Orthorhombic	Monoclinic
Space group	<i>Pnna</i>	<i>C2/c</i>
<i>a</i> (Å)	23.599 (5)	32.222 (6)
<i>b</i> (Å)	37.492 (7)	16.172 (3)
<i>c</i> (Å)	19.730 (4)	20.802 (4)
β (°)	90	92.77 (3)
<i>V</i> (Å ³)	17457 (6)	10827 (4)
Z	4	4
ρ_{calcd} , g/cm ³	1.498	1.369
μ , mm ⁻¹	3.417	2.740
R1 (F_o)	0.0481	0.0375
wR2(F_o^2)	0.1362	0.1068
GOF	1.042	1.056

Crystal Structures

Table S2. Crystallographic data for compounds $\mathbf{[4]}_{\infty} \cdot \text{CH}_2\text{Cl}_2 \cdot 1/2\text{EtOEt}$ and $\mathbf{5} \cdot \text{CH}_2\text{Cl}_2$.

Compound	$\mathbf{[4]}_{\infty} \cdot \text{CH}_2\text{Cl}_2 \cdot 1/2\text{EtOEt}$	$\mathbf{5} \cdot \text{CH}_2\text{Cl}_2$
Empirical formula	$\text{C}_{172}\text{H}_{128}\text{Ag}_4\text{Cl}_4\text{N}_2\text{OP}_4\text{Pt}_4$	$\text{C}_{179}\text{H}_{140}\text{Ag}_4\text{Cl}_2\text{N}_2\text{P}_4\text{Pt}_4$
fw	3716.28	3725.55
Temperature (K)	193.15	77(2)
radiation (λ , Å)	0.71073	0.72000
Crystal system	Orthorhombic	Monoclinic
Space group	$Pbca$	$P2(1)/c$
a (Å)	24.901(5)	18.249(4)
b (Å)	24.480(5)	14.605(3)
c (Å)	26.342(5)	27.333(6)
β (°)	90	91.31(3)
V (Å ³)	16057(6)	7283(3)
Z	4	2
ρ_{calcd} , g/cm ³	1.537	1.699
μ , mm ⁻¹	4.103	4.488
R1 (F_o)	0.0618	0.0484
wR2(F_o^2)	0.1657	0.1449
GOF	1.185	1.143

Crystal Structures

Table S3. Bond lengths and bond angles for **1·3/2CH₂Cl₂** and **3·MeCN·CH₂Cl₂**.

	bond distance [Å]				
	1·3/2CH₂Cl₂			3·MeCN·CH₂Cl₂	
Pt–C	Pt(1)-C(44)#1 Pt(1)-C(44) Pt(2)-C(4)#1	2.002(4) 2.002(4) 1.991(3)	Pt(2)-C(4) Pt(3)-C(92) Pt(3)-C(100)	1.991(3) 1.999(4) 2.002(4)	Pt(1)-C(1) 1.989(2) Pt(1)-C(21) 1.988(2)
Pt–P	Pt(1)-P(1) Pt(1)-P(1)#1 Pt(2)-P(2)	2.2883(10) 2.2883(10) 2.2822(11)	Pt(2)-P(2)#1 Pt(3)-P(3) Pt(3)-P(4)	2.2823(11) 2.2853(9) 2.2832(10)	Pt(1)-P(1) 2.2908(7) Pt(1)-P(2) 2.2845(7)
	bond angle [°]				
C–Pt–C	C(44)#1-Pt(1)-C(44) C(4)-Pt(2)-C(4)#1 C(92)-Pt(3)-C(100)	179.19(19) 178.7(2) 178.00(16)	C(1)-Pt(1)-C(21)	173.29(10)	
P–Pt–P	P(1)-Pt(1)-P(1)#1 P(2)-Pt(2)-P(2)#1 P(4)-Pt(3)-P(3)	173.94(4) 176.17(4) 175.18(3)	P(2)-Pt(1)-P(1)	177.98(2)	
C–Pt–P	C(44)#1-Pt(1)-P(1) C(44)-Pt(1)-P(1) C(44)#1-Pt(1)-P(1)#1 C(44)-Pt(1)-P(1)#1 C(4)#1-Pt(2)-P(2) C(4)-Pt(2)-P(2) C(4)-Pt(2)-P(2)#1 C(4)#1-Pt(2)-P(2)#1 C(92)-Pt(3)-P(3) C(92)-Pt(3)-P(4) C(100)-Pt(3)-P(3)	93.45(11) 86.51(11) 86.51(11) 93.44(11) 87.16(12) 92.88(12) 87.16(12) 92.88(12) 93.42(13) 86.80(13) 84.69(10)	C(1)-Pt(1)-P(1) C(1)-Pt(1)-P(2) C(21)-Pt(1)-P(1) C(21)-Pt(1)-P(2)	87.68(7) 90.35(7) 93.80(7) 88.21(7)	

Symmetry transformations used to generate equivalent atoms: #1 -x+3/2,-y+1, z

Crystal Structures

Table S4. Bond lengths and bond angles for $\mathbf{[4]}_{\infty}\cdot\text{CH}_2\text{Cl}_2\cdot1/2\text{EtOEt}$ and $\mathbf{5}\cdot\text{CH}_2\text{Cl}_2$.

	bond distance [Å]					
	$\mathbf{[4]}_{\infty}\cdot\text{CH}_2\text{Cl}_2\cdot1/2\text{EtOEt}$			$\mathbf{5}\cdot\text{CH}_2\text{Cl}_2$		
Pt–Ag	Pt(1)-Ag(1) 3.1807(10)	Pt(2)-Ag(1) 2.9198(9)	Pt(1)-Ag(2) 3.0122(9)	Pt(1)-Ag (1) 3.0831(9)	Pt(2)-Ag(1) 3.0062(9)	Pt(2)-Ag(2) 3.0317(6)
	Pt(1)-Ag(2) 2.9078(8)	Pt(2)-Ag(2) 3.0122(9)	Pt(1)-Ag(2) 3.0161(9)	Pt(2)-Ag(2) 3.0317(6)		
Pt–P	Pt(1)-P(2) 2.299(2)	Pt(2)-P(1) 2.307(2)	Pt(1)-P(2) 2.2994(11)	Pt(2)-P(1) 2.2933(10)		
Pt–C	Pt(1)-C(1) 2.019(10)	Pt(2)-C(31) 2.030(10)	Pt(1)-C(1) 2.013(4)	Pt(2)-C(11) 2.021(4)		
	Pt(1)-C(11) 2.007(9)	Pt(2)-C(41) 2.008(10)	Pt(1)-C(21) 2.010(4)	Pt(2)-C(31) 2.008(4)		
	Pt(1)-C(21) 2.023(9)	Pt(2)-C(51) 1.998(10)	Pt(1)-C(51) 2.018(4)	Pt(2)-C(41) 1.999(4)		
Ag–C	Ag(1)-C(1) 2.334(9)	Ag(2)-C(11) 2.696(9)	Ag(1)-C(11) 2.259(4)	Ag(2)-C(1) 2.490(4)		
	Ag(1)-C(21) 2.658(9)	Ag(2)-C(21) 2.604(10)	Ag(1)-C(21) 2.283(4)	Ag(2)-C(31) 2.291(4)		
	Ag(1)-C(41) 2.277(10)	Ag(2)-C(51) 2.473(9)	Ag(1)-C(12) 2.514(4)	Ag(2)-C(51) 2.413(4)		
	Ag(1)-C(2) 2.501(9)		Ag(1)-C(22) 2.402(4)	Ag(2)-C(32) 2.545(4)		
	Ag(1)-C(42) 2.622(11)			Ag(2)-C(52) 2.626(4)		
Ag–N	Ag(2)-N(1)#1 2.290(7)					
C–C	C(1)-C(2) 1.220(13)	C(31)-C(32) 1.164(13)	C(1)-C(2) 1.217(6)	C(31)-C(32) 1.225(6)		
	C(11)-C(12) 1.195(13)	C(41)-C(42) 1.216(15)	C(11)-C(12) 1.218(6)	C(41)-C(42) 1.211(6)		
	C(21)-C(22) 1.217(14)	C(51)-C(52) 1.210(13)	C(21)-C(22) 1.223(6)	C(51)-C(52) 1.214(6)		
	bond angle [°]					
C–Pt–C	C(1)-Pt(1)-C(21) 88.3(4)	C(41)-Pt(2)-C(31) 86.9(4)	C(1)-Pt(1)-C(51) 87.48(17)	C(31)-Pt(2)-C(11) 90.75(16)		
	C(11)-Pt(1)-C(21) 89.9(4)	C(51)-Pt(2)-C(31) 88.0(4)	C(21)-Pt(1)-C(1) 88.68(17)	C(41)-Pt(2)-C(11) 87.81(16)		
	C(11)-Pt(1)-C(1) 177.0(4)	C(51)-Pt(2)-C(41) 170.4(4)	C(21)-Pt(1)-C(51) 172.27(16)	C(41)-Pt(2)-C(31) 174.84(16)		
C–Pt–P	C(1)-Pt(1)-P(2) 88.3(3)	C(41)-Pt(2)-P(1) 93.6(3)	C(51)-Pt(1)-P(2) 89.15(13)	C(41)-Pt(2)-P(1) 87.17(11)		
	C(11)-Pt(1)-P(2) 93.9(3)	C(51)-Pt(2)-P(1) 92.8(2)	C(21)-Pt(1)-P(2) 93.97(12)	C(31)-Pt(2)-P(1) 94.31(12)		
	C(21)-Pt(1)-P(2) 172.4(3)	C(31)-Pt(2)-P(1) 170.4(3)	C(1)-Pt(1)-P(2) 173.32(12)	C(11)-Pt(2)-P(1) 174.94(12)		
C–Ag–C	C(1)-Ag(1)-C(21) 68.3(3)	C(21)-Ag(2)-C(11) 64.9(3)	C(11)-Ag(1)-C(21) 160.43(16)	C(51)-Ag(2)-C(1) 69.26(14)		
	C(21)-Ag(1)-C(41) 128.2(3)	C(51)-Ag(2)-C(11) 128.5(3)	C(21)-Ag(1)-C(12) 146.22(15)	C(31)-Ag(2)-C(1) 130.07(14)		
	C(41)-Ag(1)-C(1) 155.1(3)	C(51)-Ag(2)-C(21) 137.2(3)		C(31)-Ag(2)-C(51) 155.0(1)		
N–Ag–C	N(1)#1-Ag(2)-C(11) 92.4(3)					
	N(1)#1-Ag(2)-C(21) 100.1(3)					
	N(1)#1-Ag(2)-C(51) 117.3(3)					

Photophysical Properties

Electronic absorption spectra

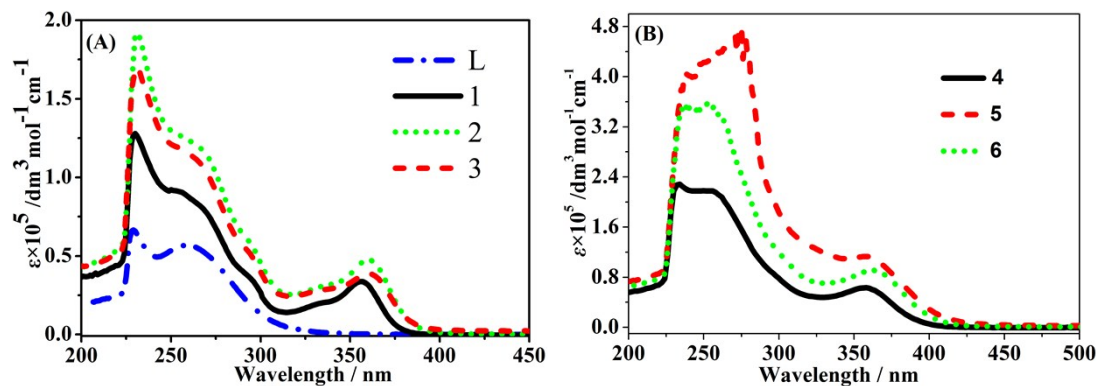


Fig. S3 The electronic absorption spectra of L ligand, **1-3** (A) and **4-6** (B) in CH_2Cl_2 solution at room temperature.

Photophysical Properties

Emission spectra

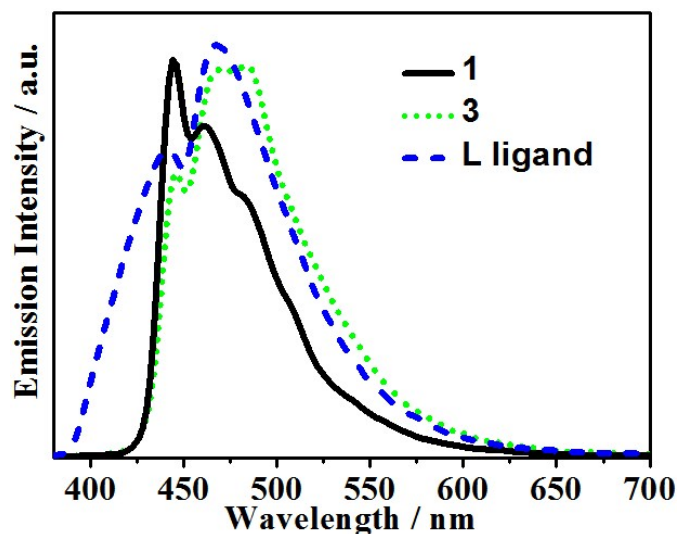


Fig. S4 Emission spectra of compounds **1**, **3** and L ligand in the solid state at 298 K.

Photophysical Properties

Emission spectra

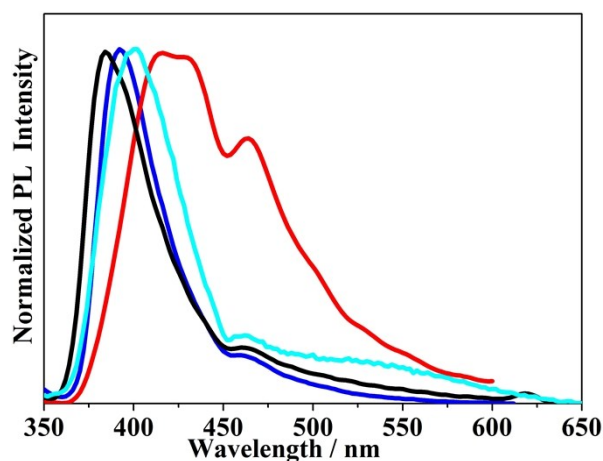


Fig. S5 Emission ($\lambda_{\text{ex}} = 312 \text{ nm}$) spectra of compounds **1** (black line), **2** (red line), **3** (blue line) and L (cyan line) ligand in CH_2Cl_2 (298 K) with the concentration $1 \times 10^{-4} \text{ M}$.

Photophysical Properties

Computational Details

All the calculations were carried out by using the Gaussian 09 program package¹ to get insight into the photophysical properties of [4]_∞. The initial structure was extracted from the crystallographically determined geometry. To analyze the emission properties of the cluster, one hundred triplet excited states were calculated by the time-dependent DFT (TD-DFT)^{2, 3} method at the gradient corrected correlation functional PBE1PBE⁴ level on the basis of the ground state geometry structure. In these calculations, the Hay-Wadt double- ζ with a Los Alamos relativistic effect basis set (LANL2DZ)^{5, 6} consisting of the effective core potentials (ECP) was employed for the Ag and Pt atoms, and 6-31G* basis set for the remaining non-metal atoms. Visualization of the frontier molecular orbitals was performed by GaussView software⁷. In the Multiwfn⁸ program package, Ros-Schuit method⁹ (C-squared population analysis method, SCPA) was supported to analyze the partition orbital composition.

Photophysical Properties

Table S5. Partial molecular orbital compositions (%) in the triplet excited state for the simplified model of $[4]_\infty$ in solid state by TD-DFT method at the PBE1PBE level.

orbital	energy (eV)	MO contribution (%)			
		Ag	Pt	C≡CR	L
LUMO+9	-0.027	32.72	10.31	33.30	23.67
LUMO+8	-0.136	51.42	6.80	14.96	26.82
LUMO+1	-2.721	2.01	2.27	1.17	94.55
HOMO	-4.054	45.36	4.32	21.11	29.21
HOMO-4	-6.041	13.91	35.51	50.55	0.03

Table S6 The excitation transitions for the simplified model of $[4]_\infty$ in solid state by TD-DFT method at the PBE1PBE level.

states	E , nm (eV)	O.S.	transition	contrib.	assignment
T ₁	434 (2.85)	0.0026	HOMO-4→LUMO+1	91.42%	³ MMLCT/ ³ LLCT
T ₂	354 (3.50)	0.2015	HOMO→LUMO+9	70.11%	³ MMLCT/ ³ LMMCT/ ³ IL/ ³ LLCT
			HOMO→LUMO+8	26.52%	³ MMLCT/ ³ LMMCT/ ³ IL/ ³ LLCT

Photophysical Properties

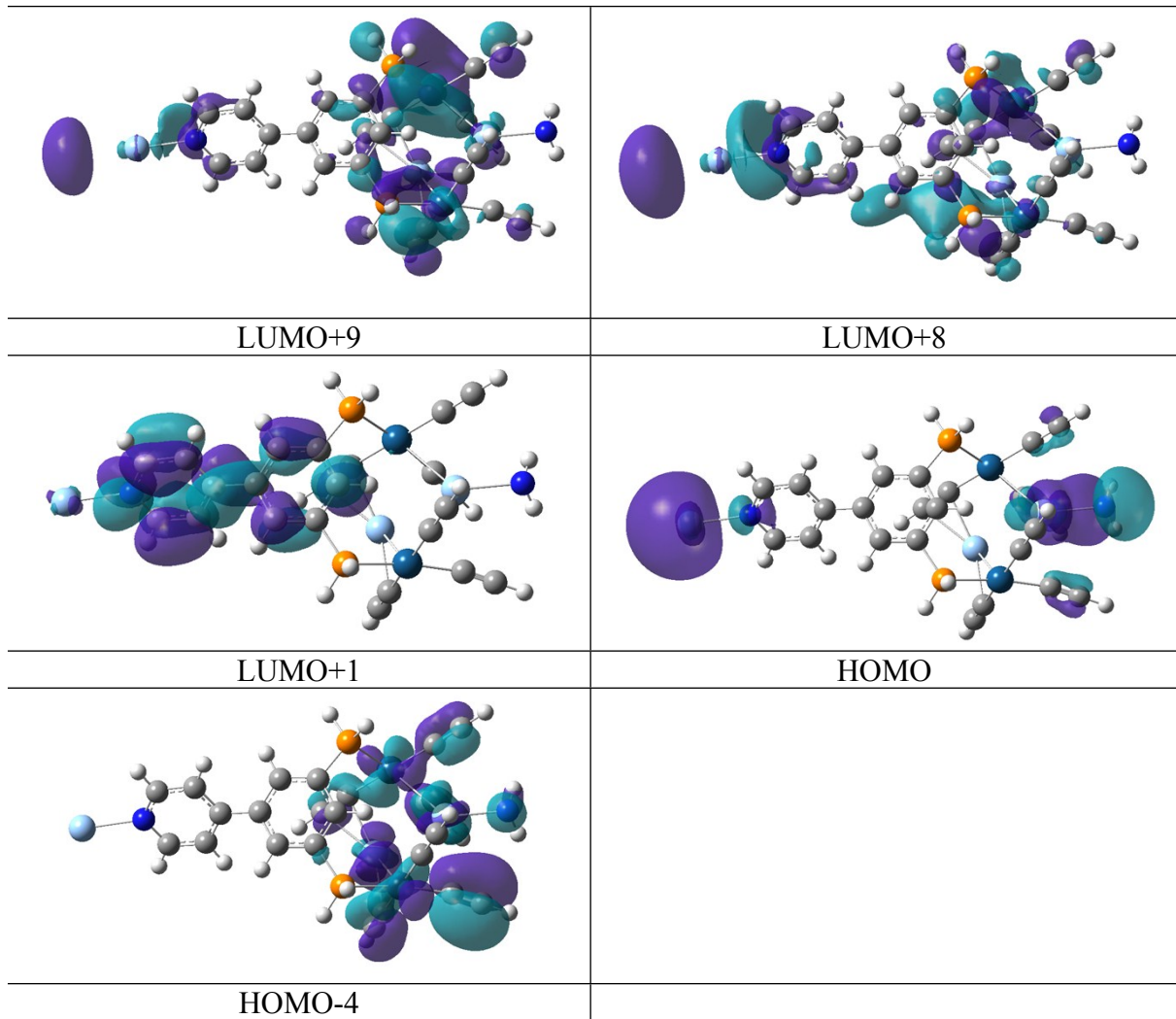


Fig. S6. Plots of the frontier molecular orbitals involved in the excitation transitions of the simplified model of $[4]_{\infty}$ in solid state by TD-DFT method at the PBE1PBE level. The cyan, royalblue, orange, blue, gray, and white spheres represent the silver, platinum, phosphorus, nitrogen, carbon, and hydrogen atoms, respectively.

Photophysical Properties

Emission spectra

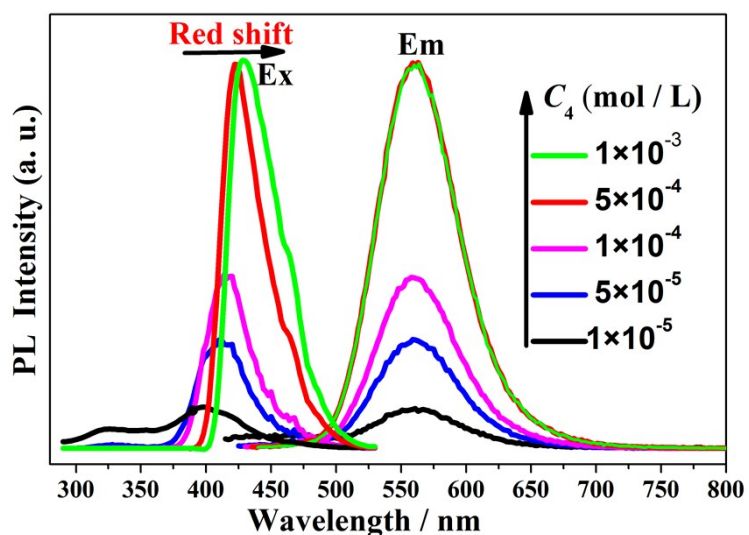


Fig. S7 Variation of the excitation (left, $\lambda_{\text{em}} = 560$ nm) and emission (right, independent of the λ_{ex} used) spectra of **4** in $\text{ClCH}_2\text{CH}_2\text{Cl}$ (298 K) with the concentration 1×10^{-5} M (black), 5×10^{-5} M (blue), 1×10^{-4} M (magenta), 5×10^{-4} M (red), and 1×10^{-3} M (green).

References

1. M. Frisch, G. Trucks, H. Schlegel, G. Scuseria, M. Robb, J. Cheeseman, G. Scalmani, V. Barone, B. Mennucci and G. Petersson, *Inc., Wallingford, CT*, 2009.
2. R. Bauernschmitt and R. Ahlrichs, *Chemical Physics Letters*, 1996, **256**, 454-464.
3. R. Stratmann, G. Scuseria and M. Frisch, *The Journal of Chemical Physics*, 1998, **109**, 8218-8224.
4. J. Perdew, K. Burke and M. Ernzerhof, *Physical review letters*, 1996, **77**, 3865-3868.
5. P. Hay and W. Wadt, *The Journal of Chemical Physics*, 1985, **82**, 299-310.
6. P. Hay and W. Wadt, *The Journal of Chemical Physics*, 1985, **82**, 270-283.
7. R. Dennington, T. Keith and J. Millam, *Semicem Inc., Shawnee Mission, KS*, 2009.
8. T. Lu and F. Chen, *Journal of computational chemistry*, 2012, **33**, 580-592.
9. P. Ros and G. Schuit, *Theoretica Chimica Acta*, 1966, **4**, 1-12.